Sensitivity of the MnTe valence band to orientation of magnetic moments

Paulo E. Faria Junior,[1] Koen A. de Mare,[2] Klaus Zollner,[1]
Sigurdur I. Erlingsson,[3] Mark van Schilfgaarde,[4] and Karel Výborný[5]

[1]*Institute for Theoretical Physics, University of Regensburg, D–93040 Regensburg, Germany*
[2]*Eindhoven University of Technology, Eindhoven NL–5612 AZ, Netherlands*
[3]*Department of Engineering, Reykjavik University, Menntavegi 1, IS-102 Reykjavik, Iceland*
[4]*King's College London, London WC2R 2LS, United Kingdom*
[5]*FZU – Institute of Physics of the Czech Academy of Sciences, Cukrovarnická 10, Praha 6, CZ–16253*
(Dated: Apr06, 2022)

An effective model of the hexagonal (NiAs-structure) manganese telluride valence band in the vicinity of the A-point of the Brillouin zone is derived. It is shown that while for the usual antiferromagnetic order (magnetic moments in the basal plane) band splitting at A is small, their out-of-plane rotation enhances the splitting dramatically (to about 0.5 eV). We propose extensions of recent experiments (Moseley et al., Phys. Rev. Materials 6, 014404) where such inversion of magnetocrystalline anisotropy has been observed in Li-doped MnTe, to confirm this unusual sensitivity of a semiconductor band structure to magnetic order.

I. INTRODUCTION

Electronic structure of crystalline semiconductors can be treated by various methods which differ greatly in their computational cost.[1] Among *ab initio* methods, GW is one of the most advanced approaches yet a numerically rather expensive one.[2] A widely-used alternative is the density functional theory (DFT) where the speed comes at the cost of worse performance (even if there are various approaches to mitigate deficiencies such as too small gaps) and yet faster options are available, of which tight-binding approaches[3] and $k \cdot p$ models[4] will be of interest here. Such effective models need material parameters (such as on-site energies or hopping amplitudes) as an input which can sometimes be of advantage because they can be adjusted to fit experiments.

An archetypal example of an effective model is the Kohn-Luttinger Hamiltonian[5] which has a wide range of applications to non-magnetic materials, including silicon and III-V semiconductors with Γ_8 manifold at the top of the valence band (VB). Magnetism adds a new twist: for Mn-doped GaAs, the host is described by this Hamiltonian and the effect of ferromagnetic ordering is captured by a kinetic pd exchange term $\propto \hat{\vec{s}} \cdot \vec{S}$ where $\hat{\vec{s}}$ is the spin operator (of the VB holes) and $\vec{S}$ is the classical spin representing the Mn magnetic moments (usually treated on the mean-field level). Such description of ferromagnetic semiconductors[6,7] has been employed extensively in the context of spintronics[8] and now that *antiferromagnetic* spintronics[9] has become an active field, we hereby wish to contribute to its progress by presenting an effective model of hexagonal (NiAs-structure) MnTe which is a well-established antiferromagnetic semiconductor, as exemplified by its $T = 0$ band structure in Fig. 1, with a relatively high (≈ 310 K) Néel temperature. Typical samples, both bulk and layers exhibit p-type conductivity and we will therefore focus on its valence band (VB).

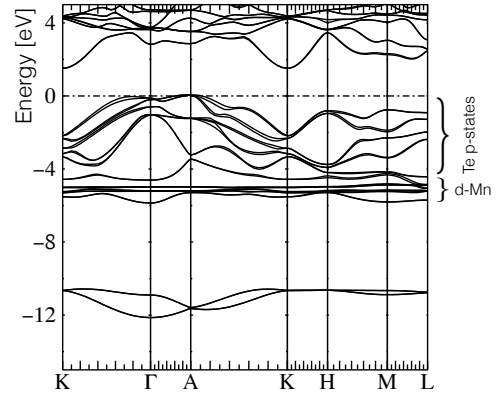Magnetic structure of MnTe was established[10] long ago (see Fig. 2) with a strong anisotropy favouring in-plane

FIG. 1. Band structure of MnTe calculated by QSGW. Note the competing maxima of the valence band at Γ and A points.

orientation of the magnetic moments and a weak residual anisotropy within the plane.[11] Recently, Moseley et al.[13] have found by neutron diffraction that, upon doping by lithium, the magnetic moments rotate out of plane. They also noticed that, on the level of density of states (DOS), significant changes occur and we use the effective model to explain how the VB responds to this change of magnetic order (once spin-orbit interaction is taken into account). Even if the Mn d-states lie[12] deep below the Fermi level E_F seem too remote from the VB top, which is built dominantly from p-Te orbitals, we demonstrate that the combination of MnTe layered structure and the spin-orbit interaction (SOI) lead to an unusual sensitivity of the electronic structure to the orientation of magnetic moments. In the next Section we discuss the competing VB maxima and we focus on the one near A-point of the Brillouin zone (BZ) in Sec. III. We conclude in Sec. IV.

II. COMPETING VB MAXIMA

Once the SOI is taken into account, there arises a tight competition between valence band maxima close to A and Γ points of the BZ, see Fig. 2b. A long-standing consensus[14,15] that the former prevails has recently been challenged by Yin et al. [18] who claim that the VB top occurs in the vicinity of Γ point. To improve on the potentially less accurate DFT approach,[18] we employ the Quasiparticle Self-Consistent GW approximation[16] (QSGW). The GW approximation, which is an explicit theory of excited states is widely used to predict quasiparticle levels with better reliability than density functionals. QSGW is an optimized form of the GW approximation, where the starting hamiltonian is generated within the GW approximation itself, constructed so that it minimizes the difference between the one-body and many-body hamiltonians. As a by-product the poles of the one-body Green's function coincide with the poles of the interacting one: thus energy band structures have physical interpretation as quasiparticle levels, in marked contrast to DFT approaches where the auxillary hamiltonian has no formal physical meaning (in practice Lagrange multipliers of this hamiltonian are interpreted as quasiparticle levels). In practice QSGW yields high fidelity quasiparticle levels in most materials where dynamical spin fluctuations are not strong.[17]

Bulk lattice constants of MnTe at room temperature are $a = 0.414$ nm and $c = 0.671$ nm; we show in Fig. 2d that for such $c/a = 1.621$, the VB maximum close to the A point safely prevails (ΔE is the difference between energy of local VB maxima close to Γ and that close to A). Most experiments nowadays are performed with thin films of MnTe, however, and then lattice constants depend on the choice of substrate. Temperature-dependent data in Fig. 3 of Ref. 11 suggest that while samples grown on SrF_2 surface still fall into the same class, low temperatures may effectively push the VB maxima close to the Γ point up and in particular, samples grown on the InP substrate may exhibit the inverted alignment of the VB maxima.

Comparing the present QSGW results to DFT calculations of Ref. 18, several remarks are in order. Lattice constants used in that reference (which correspond to $c/a = 1.57$) have been obtained by structure optimisation in DFT rather than from experimental data. Next, the hybrid functional HSE06 may avoid the known problem of underestimated gaps in DFT but this in itself does not guarantee a reliable description of finer details of the band structure (such as VB maxima alignment). Predicted valence and conduction bands are more uniformly reliable in GW than in density-functional methods. Moreover QSGW surmounts the problematic starting-point dependence that plagues the usual implementations of the GW approximation and therefore QSGW is a better choice for our study than DFT. Regarding the subsequent derivation of an effective model,[18] we note as follows. The $k_z = 0$ approximation is used;
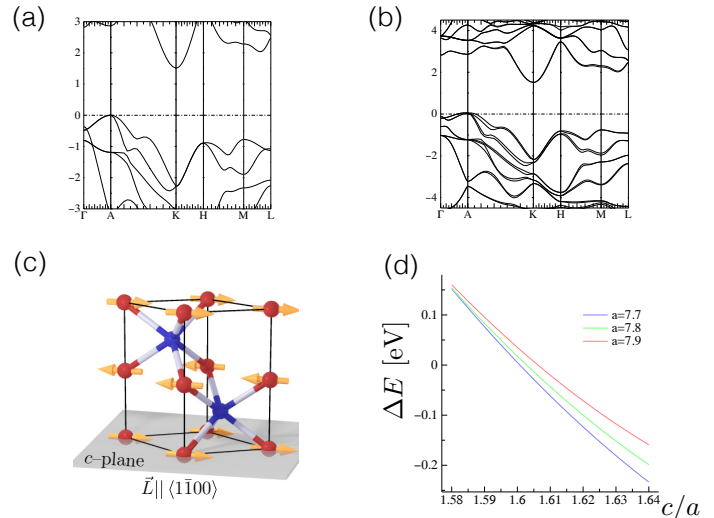

FIG. 2. Top of the valence band studied by QSGW and (c) crystal structure of MnTe. Panels (a,b) show the difference between SOI ignored and included and (d) gives for the latter case the energy difference between VB maximum in Γ and A depending on the crystal lattice parameters. Negative ΔE means that the VB maxima around A prevail. *Note:* 0.414 nm correspons to 7.81 a.u.

while this would be appropriate for very thin layers (say 5 nm), present experiments[11] are more likely behaving like 3D bulk. Also, the effective model (1) in Ref. 18 assumes a fixed direction of the magnetic moments; to plot the experimentally relevant 'angular sweeps', the current direction rather than Néel vector is rotated which is, however, not the actual experimental protocol. For systems where only the non-crystalline anisotropic magnetoresistance (AMR) occurs,[20] the two protocols are equivalent but measurements in the Corbino geometry[11] prove this assumption false. Being aware of these issues, we strive to derive an effective model in the following which captures the dependence on magnetic moments direction.

A proper symmetry analysis of the crystal structure of MnTe provides the non-symmorphic space group D_{6h}^4. Once AF ordering is included the Mn atoms must be treated as inequivalent since each Mn layer would have spins pointing in the opposite direction as shown in Fig. 2c for in-plane spins. Hence, the symmetry group is reduced from D_{6h} to D_{3d} without SOI (see for instance Sandratskii et al.[21]). Furthermore, the symmetry group would also depend on the interplay of SOI and choice of the AF direction since spins pointing in different directions behave differently under symmetry operations. For example, in the out-of-plane AF configuration, the symmetry remains D_{3d} while for in-plane AF, either along $[10\bar{1}0]$ or $[11\bar{2}0]$ directions, the symmetry group is reduced C_{2h}. Besides the conceptual analysis of the symmetries, independent calculations using the WIEN2k and Quantum Espresso ab initio packages also provide the

same symmetry groups discussed above. Thus, for the particular choice of in-plane AF the D_{2h} point group discussed by Yin et al. should be replaced by C_{2h}.

III. EFFECTIVE MODELS

Several attempts to describe the electronic structure of α-MnTe in a simplified way have been made so far. Here, the $k \cdot p$ approach[4,22] is a common choice for semiconductors[23] especially if only high-symmetry points in the BZ are of interest. Such a model for the VB top in A point was derived more than 40 years ago[21] and later extended to a tight-binding scheme.[24] The latter allows for the description of the energy bands over the whole BZ but neither of these models allows to analyse the dependence of electronic structure on the directions on Mn magnetic moments. In the perfectly ordered AFM phase (as in Fig. 2d) and without SOI, the Bloch functions at the top of the valence band in the A point transform as the two-dimensional irreducible representation E_g or (Γ_3^+) of the the D_{3d}. Including corrections up k^2 and no SOI (essentially given by Eq. 2 in Sandratskii et al.[21]) one would obtain the following Hamiltonian:

$$H_{kp,2\times2} = \begin{pmatrix} ak_x^2 + bk_y^2 + ck_z^2 & (a-b)k_xk_y \\ (a-b)k_xk_y & bk_x^2 + ak_y^2 + ck_z^2 \end{pmatrix}. \quad (1)$$

The parameters[25] a, b, c (in units of $\hbar^2/2m_0$) correspond to (anisotropic) effective masses and can be fitted to the ab initio calculations in Fig. 2(a). Note that while MnTe is a hexagonal crystal, this model has a continuous rotation symmetry around the z-axis. From the point of view of magnetism, this is a consequence of neglecting the spin-orbit interaction. Once SOI is included, the band dispersion will depend on the direction of magnetic moments. On the other hand, if higher order terms in $\vec{k}$ were included, the symmetry would be lowered to a hexagonal one (even w/o SOI). When $k_z = 0$, one of the eigenstates of this matrix will be parallel to $\vec{k}$ while the other will be orthogonal to $\vec{k}$.

The derivation of Eq. (1) is based solely on symmetry arguments and entails neither any explicit information about orbital composition of the corresponding Bloch states nor any parametric dependence on magnetic order. In the following, we therefore first describe a toy model capturing the essence of interplay between magnetism and orbital degrees of freedom and next, we make use of these insights to derive a realistic model of MnTe.

A. Toy model

Consider a 1D chain of alternating nonmagnetic (A) and magnetic (B) atoms depicted in Fig. 3 where only the nearest neighbours couple (the amplitude being t). The single-orbital-per-site tight-binding Hamiltonian assuming that the B-atom orbitals have on-site energies
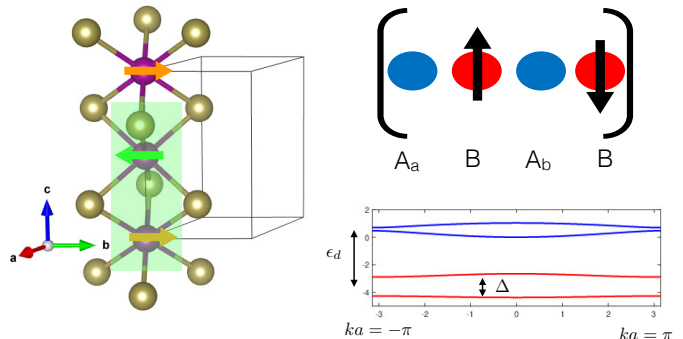

FIG. 3. The toy model: NiAs structure (left) reduced to a one-dimensional chain of magnetic (B) and non-magnetic (A) atoms. Its band structure is shown for $t = \Delta = 1$.

$\epsilon_d \pm \Delta$ (where 2Δ is the exchange splitting) reads

$$H_1(\Delta) = \begin{pmatrix} 0 & t & 0 & te^{-ika} \\ t & \epsilon_d + \Delta & t & 0 \\ 0 & t & 0 & t \\ te^{ika} & 0 & t & \epsilon_d - \Delta \end{pmatrix} \quad (2)$$

in the basis of Bloch states with momentum k so that ka ranging from $-\pi$ to π parametrises the BZ.

The toy model described by H_1 can be treated analytically (see Appendix) and there are two main observations to make at this point. First, even if $\Delta \ll \epsilon_d$ there opens a gap in the 'VB states' at the BZ edge. Size of the gap is parametrised by Δ. This allows for the insight that, inasmuch the atom A_b is sandwiched between spin-up (left) and spin-down neighbours (right), where the exchange coupling is Δ and $-\Delta$, their effect on the A-band (blue in Fig. 3 at the bottom right panel) does not average out to zero. An even more important insight concerns the eigenstates of H_1 at $ka = \pm\pi$.

At this point, we should point out that H_1 of (2) in fact only describes one of the two spin species; let us denote it as up-spin and correspondingly, $H_{1,\uparrow} = H_1(\Delta)$. The two states at $ka = \pm\pi$ split by nonzero Δ turn out to be $(|a\rangle \pm |b\rangle) \otimes |\uparrow\rangle$ where $|a\rangle$ and $|b\rangle$ refer to orbitals of A_a and A_b atoms, respectively. For the spin-down sector, $H_{1,\downarrow} = H_1(-\Delta)$ which leads to identical band structure as in Fig. 3 whose eigenstates are nevertheless not the same as for $H_{1,\uparrow}$. The state degenerate with $(|a\rangle \pm |b\rangle) \otimes |\uparrow\rangle$ is $(|a\rangle \mp |b\rangle) \otimes |\downarrow\rangle$ and thus, we arrive at the conclusion that, at the BZ edge, the VB states in our toy model come in two pairs (split by the gap) and without loss of generality, we now focus on the subspace

spanned by the pair

$$(|a\rangle + |b\rangle) \otimes |\uparrow\rangle, (|a\rangle - |b\rangle) \otimes |\downarrow\rangle. \qquad (3)$$

Unlike the pair $|\uparrow\rangle, |\downarrow\rangle$ (without any orbital part), any linear combination of the two states in (3) has a zero expectation value of transversal spin operators $\hat{\sigma}_x$, $\hat{\sigma}_y$. This can also be restated as $\langle \hat{\vec{\sigma}} \rangle \| z$, or, easily generalised to the statement that the states (3) have the (expectation value of) spin parallel to the magnetic moments of atoms B. In this way, the *direction* of magnetic moments of the atoms remote in energy from the VB top influences the current-carrying states close to the Fermi energy. In the following, we denote the direction of spin in the basis

state $(|a\rangle + |b\rangle) \otimes |\uparrow\rangle$ by $\vec{L}$ and it can be understood as the Néel vector.

B. Extension to MnTe crystal

The previous argument can be extended to Te p_x, p_y states which form the VB top near A. For reasons to be explained later, we also include the remote p_z levels (in A, they are ≈ 3 eV below the VB top, see Fig. 2a) whose dispersion is dropped at this level of approximation. We will measure energy from the VB top and with E_F being the Fermi energy. We recall Eq. (1) and take the parameters a, b, c from the fit to ab initio calculations without SOI.

Denoting the position of p_z orbitals of tellurium by e_z ($e_z < 0$, $|e_z/E_F| \gg 1$), the full description of the VB close to A is provided by a block-diagonal 6×6 matrix

$$H_{kp} = \begin{pmatrix} ak_x^2 + bk_y^2 + ck_z^2 & (a-b)k_xk_y & 0 & & & \\ (a-b)k_xk_y & bk_x^2 + ak_y^2 + ck_z^2 & 0 & & & \\ 0 & 0 & e_z & & & \\ & & & ak_x^2 + bk_y^2 + ck_z^2 & (a-b)k_xk_y & 0 \\ & & & (a-b)k_xk_y & bk_x^2 + ak_y^2 + ck_z^2 & 0 \\ & & & 0 & 0 & e_z \end{pmatrix} \qquad (4)$$

and the first and second 3×3 block is written in the basis (3) whereas inside the blocks, the basis vectors are simply $|p_x\rangle, |p_y\rangle, |p_z\rangle$. Since the matrix (4) does not explicitly depend on $\vec{L}$ (only its basis vectors are), we arrive at the conclusion that (when SOI is ignored) the band structure does not depend on the direction of Mn magnetic moments.

In the limit $|e_z| \to \infty$, the full model (4) breaks down into two decoupled 2×2 blocks (1); since we now have a microscopic understanding of the basis, one which contains the information about direction of Mn magnetic moments, the SOI can now be evaluated. Also, the usefulness of finite e_z will then become clear.

C. Spin-orbit interaction

We are now in a position to explain the following behaviour of band structure calculated by relativistic *ab initio* methods. In panel (b) of Fig. 2, we could have already observed the bands split by SOI and, compared to band widths, such splittings were small. Those calculations were done assuming $\vec{L} \| x$ and, at this level of detail, depend only little on the direction of $\vec{L}$ as long as $\vec{L} \perp z$ which is compatible with MnTe being an easy-plane material.[11] However, when $\vec{L} \| z$ is assumed in calculations, see Fig. 4, band splittings become sizable. Restricting our discussion to Te p_x, p_y orbitals combined into the states (3), this behaviour is linked to the directionality of $H_{so} = \lambda \vec{l} \cdot \vec{\sigma}$ evaluated in the corresponding basis:

$$H_{so,2\times 2} = \begin{pmatrix} 0 & i\lambda\cos\theta \\ -i\lambda\cos\theta & 0 \end{pmatrix} \qquad (5)$$

where $\vec{L} \cdot \hat{z} = \cos\theta$ and $\vec{l}$ is the orbital angular momentum operator. Clearly, SOI projected to the 'small' subspace of orbitals from which the top of the VB is composed,

completely vanishes when Mn magnetic moments are in-plane, i.e. $\vec{L} \cdot \hat{z} = 0$. The small band splittings at A seen in Fig. 2(b) come from states lying further away in energy, i.e. finite $|e_z|$ as discussed in the appendix. As soon as $\vec{L}$ acquires an out-of-plane component, splittings $\propto \lambda$ are possible.

IV. DISCUSSION AND CONCLUSIONS

The minimal description of the valence band in MnTe comprises two identical copies of terms (1) and (5) added; it means that all bands remain double degenerate at this level of approximation. Higher order terms are necessary to lift this degeneracy (which is actually observed in ab initio calculations along directions of low symmetry). Splittings occuring at A (nearly absent for in-plane magnetic moments and ≈ 0.5 eV for $\vec{L} \| z$) are qualitatively reproduced using the 6×6 model (4) combined with SOI of the form $\lambda \vec{l} \cdot \vec{\sigma}$; a quantitative description requires, however, anisotropic SOI with $\lambda_{xy}/\lambda_z \approx 0.22$.

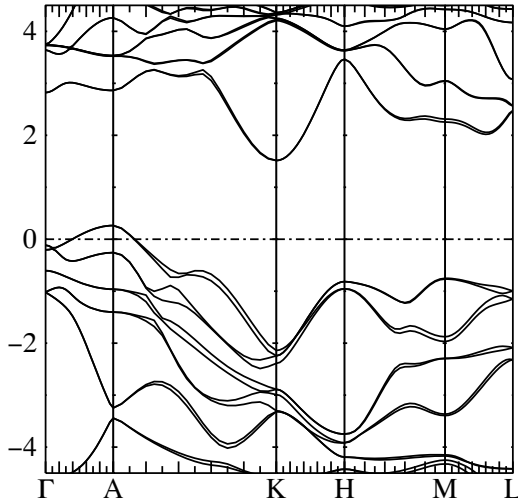Calculations in Fig. 4 show that the splitting at A is associated with reduction of band gap in agreement with

FIG. 4. MnTe band structure for $\vec{L}||z$.

DFT calculations.[13] This implies that not only angular-resolved photoemission (ARPES) could be used to confirm the sensitivity of MnTe band structure to the orientation of Mn magnetic moments but also optical absorption measurements should reveal signatures of this effect.

Appendix A: Analytical results concerning (2)

Toy model (2) can be rearranged into the block form

$$H = \begin{pmatrix} A & C \\ C^+ & B \end{pmatrix}, \qquad C = \begin{pmatrix} t & te^{-ika} \\ t & t \end{pmatrix}$$

with $B = 0$ and A diagonal $\epsilon_d \pm \Delta$. Downfolded matrix corresponding to basis $|a\rangle, |b\rangle$ then reads

$$H_{eff} = -\frac{2\epsilon_d t^2}{\epsilon_d^2 - \Delta^2} \begin{pmatrix} 1 & \alpha(k) \\ \alpha^*(k) & 1 \end{pmatrix} \qquad (A1)$$

where $\alpha(k) = e^{-ika/2}(\cos ka + i\delta \sin ka)$ and we assumed $\delta = \Delta/\epsilon_d \ll 1$.

Appendix B: More on spin-orbit

Since there's a small splitting in A also when $\vec{L}$ is in-plane, we need to consider finite e_z in (4) rather than $|e_z| \to \infty$

Next, explain

$$H_{so} = \lambda_z S_z L_z + \lambda_{xy}(S_x L_x + S_y L_y) \qquad (B1)$$

and give $\lambda_z = 0.27$ eV and $\lambda_{xy} = 60$ meV; for $|e_z| \to \infty$, the $|p_z\rangle$ subspace can be ignored and H_{so} reduces to Eq. 5 with $\lambda = \lambda_z$. When e_z is finite and mag. moments are in-plane, the splitting is given by λ_{xy}.

The off-diagonal blocks in (4) only become non-zero away from the A point once basis (3) changes and its two elements are no longer orthogonal.

[1] Fabien Tran et al., J. Appl. Phys. 126, 110902 (2019)

[2] M. Grumet et al., Phys. Rev. B 98, 155143 (2018).

[3] O.K. Andersen and O. Jepsen, Phys. Rev. Lett. 53, 2571 (1984).

[4] R. Winkler, *Spin-orbit Coupling Effects in Two-Dimensional Electron and Hole Systems*, (Springer, New York, 2003).

[5] J. M. Luttinger, Phys. Rev. 102, 1030 (1956).

[6] M. Tanaka, Jpn. J. Appl. Phys. 60, 010101 (2021).

[7] T. Jungwirth et al., Rev. Mod. Phys. 86, 855 (2014).

[8] C.H. Marrows and B.J. Hickey, Phil. Trans. R. Soc. A 369, 3027 (2011).

[9] V. Baltz et al., Rev. Mod. Phys. 90, 015005 (2018).

[10] T. Komatsubara et al. '63, doi: 10.1143/JPSJ.18.356

[11] D. Kriegner et al., Phys. Rev. B 96, 214418 (2017).

[12] H. Sato et al., Sol. St. Comm. 92, 921 (1994).

[13] D.H. Moseley et al., Phys. Rev. Mat. 6, 014404 (2022).

[14] M. Podgorny and J. Oleszkiewicz, J. Phys. C: Sol. St. Phys. 16, 2547 (1983).

[15] More recent studies include S. J. Youn et al., phys. stat. sol. (b) 241, 1411 (2004) or Ref. 11.

[16] T. Kotani et al., Phys. Rev. B 76, 165106 (2007).

[17] M. van Schilfgaarde and Takao Kotani and S. Faleev, Phys. Rev. Lett. 96, 226402 (2006).

[18] G. Yin et al., Phys. Rev. Lett. 122, 106602 (2019).

[19] Apart from the NiAs-type structure of MnTe, zinc-blende phase also exists which is AFM at low temperatures.

[20] A.W. Rushforth et al., Phys. Rev. Lett. 99, 147207 (2007).

[21] L.M. Sandratskii et al. '81, doi: 10.1002/pssb.2221040111

[22] L. C. Lew Yan Voon, M. Willatzen, *The k · p method: electronic properties of semiconductors*, (Springer, Berlin, 2009).

[23] P. E. Faria Junior, T. Campos, C. M. O. Bastos, M. Gmitra, J. Fabian, and G. M. Sipahi, Phys. Rev. B **93**, 235204 (2016).

[24] J. Mašek et al. '87, doi: 10.1088/0022-3719/20/1/010

[25] The *d*-term used in Ref. 21 has been omitted.